Robust Frame Boundary Synchronization for In-Band Full-Duplex OFDM System

Sergey Shaboyan, Alireza S. Behbahani, Ahmed M. Eltawil
Department of Electrical Engineering and Computer Science, University of California Irvine
Irvine, California 92617, USA
Email: {sshaboya, sshahanb, aeltawil}@uci.edu

***Abstract*—This paper presents a robust frame boundary synchronization technique for In-Band Full-Duplex (IBFD) communication systems, that employ Orthogonal Frequency Division Multiplexing (OFDM). First, we describe the system model of a wireless link consisting of a full-duplex (FD) base station, that is receiving a signal from a remote station while transmitting simultaneously on the same frequency. Received signal impairments such as carrier frequency offset (CFO), sampling time offset (STO), channel response and channel delay are modeled. We then identify two common scenarios that can occur and cause the correlation base frame edge detection to fail. We present a novel and robust frame start detection technique taking into account STO, CFO and channel estimation effects. Performance of the proposed technique is quantified using a simulation framework and confirmed using experimental measurements. The proposed robust synchronization method demonstrated successful frame edge detection with up to 65 ppm carrier frequency offset versus a loss of 40% of the frames without using the proposed method.**

Keywords*—*In-Band, Full-Duplex, Self-Interference, Suppression, Synchronization, Interferer, Wireless Network

I. Introduction

Recently Full-Duplex (FD) communication has gained significant interest due to demonstrable increase in throughput and spectral efficiency. Conventional Half-duplex (HD) communication systems use either time-duplexing or frequency-duplexing to avoid self-interference [1]. In contrast full-duplex systems transmit and receive simultaneously on the same frequency band, thus optimally utilizing available resources. The main challenge in FD systems is managing the self-interference (SI) signal at each node, which is typically orders of magnitude larger than the intended Signal of Interest (SOI). To achieve sufficient SI suppression FD systems rely on cancellation across multiple domains (spatial, analog and digital cancellation).

Coupling FD with Orthogonal Frequency Division Multiplexing (OFDM) is a logical step towards achieving high spectral efficiency. However, the performance of OFDM-based FD systems can be substantially degraded due to frequency synchronization errors between transmitter and receiver [1]. Synchronization of wireless nodes employing OFDM has been studied by [2], and synchronization error compensation techniques were proposed assuming perfect channel state information. To estimate channel under severe timing and frequency offsets, the authors in [3] have proposed a customized frame structure of alternating pilots pre/post appended with guard intervals. A modified WiFi frame structure supporting synchronization using insertion of guard intervals has been proposed in [1] as well, however insertion of guard intervals alone is insufficient for robust frame boundary detection. Under scenarios of severe time drift or substantially large SI, frame start detection fails to detect the correct edge causing incorrect placement of Fast Fourier Transform (FFT) window resulting in ISI and ICI as will be discussed in Section IV.

Since frame boundary detection is the first crucial step in the synchronization chain, in this paper we will focus on identifying and analyzing the scenarios causing block boundary detection failure in FD mode. We then propose a technique enabling successful block boundary detection even under severe offsets. In particular, the paper presents the following contributions:

- A novel block boundary detection technique relaxing requirement of guard interval separating short training sequences and boosting robustness of frame start detection algorithm is proposed.
- A novel receiver architecture is presented for simultaneous SI cancellation and STO/CFO impairment recovery.
- Performance of the system impacted by dynamic channel effects and synchronization errors is evaluated using Matlab simulation as well as experimentally on the real-time FD platform.

The remainder of the paper is organized as follows. In Section II an IBFD system combined with OFDM is described. In Section III sources of timing and frequency misalignment effects are described and their impacts on SI cancellation are highlighted. In Section V, robust block boundary detection technique (RBBD) of both SI and SOI is proposed. Functionality of RBBD is demonstrated experimentaly in Section VI. Performance results of simulated system under different channel conditions is presented and compared in Section VII. The paper is concluded in Section VIII.

1) Notation: We use $(*)$ to denote convolution, $(.)^*$ to denote conjugate, and $arg[.]$ to denote argument of a complex number. Time domain variables are represented as lowercase letters, while frequency domain variables use uppercase. Furthermore, bold lowercase letters denote vectors.

II. System Model

Figure 1 illustrates a wireless system operating in full-duplex mode. The system consists of base station (BS) receiving from a remote node, at the same time transmitting to another node on the same frequency band. Signals transmitted

by the remote node to the base station are referred to as SOI. The transmitted signal by the base station causes SI, therefore the received signal by the base station in the time domain can be modeled as

$$r(t) = s^{rx}(t) + y^{rx}(t) + w(t) \quad (1)$$

where $s^{rx}(t)$, $y^{rx}(t)$ are SOI and SI components of the received signal, and $w(t)$ is Additive White Gaussian Noise (AWGN).

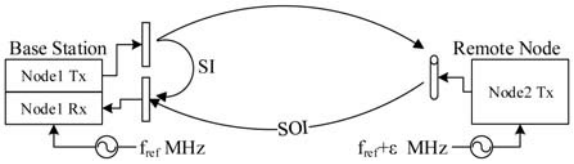

Fig. 1: Diagram of full duplex relayed Wi-Fi Network.

From Eq. (1) it is clear that SI must be suppressed in order to achieve satisfactory SINR for the received signal.

Numerous techniques are available for SI suppression, including passive (eg. antenna separation, directional antennas etc.) and active (analog and digital cancellation). Both analog and digital cancellation techniques rely on subtraction of the local copy of SI in analog or digital domains respectively [4].

A. Transmitter

All nodes use packetized data transmission, where every data packet starts with a header consisting of training sequences. Training is divided into short and long preambles using similar structure as standard WiFi [5]. Both the base station Tx and the remote node Tx are using modified non-overlapping training fields to support IBFD synchronization as described in [1]. A guard time (Trans) is inserted by the transmitter between long training fields and populated by zero vectors to protect them from overlapping due to the time drift [3]. Short training fields are not separated by zero vectors, by virtue of proposed boundary detection technique that can tolerate partial overlap without performance degradation, which is discussed in details in Section IV. The data symbols of both Tx frames are fully overlapping.

All nodes use OFDM that employs N_{FFT} subcarriers with inter-carrier spacing Δf. For sampling frequency f_s, subcarrier spacing is computed as

$$\Delta f = \frac{f_s}{N_{FFT}} = \frac{1}{N_{FFT}T_s} = \frac{1}{T_{sym}} \quad (2)$$

where T_s is sampling period, f_s is sampling frequency and T_{sym} is one OFDM symbol duration.

At the transmitter, for the i^{th} dataset, vector $\boldsymbol{d_i}$ consisting of N_d data symbols and M pilots is constructed and modulated on the $N_{FFT} = N_d + M$ subcarriers using Inverse Fast Fourier Transform (IFFT), forming one OFDM symbol. The output of IFFT is collected into vector $\boldsymbol{z_i}$=$[z_i(0), z_i(1), ..., z_i(N_{FFT} - 1)]^T$, where

$$z_i(n) = \begin{cases} \frac{1}{N_{FFT}} \sum_{k=0}^{N_{FFT}-1} d_i(k) e^{\frac{j2\pi kn}{N_{FFT}}} & 0 \le n < N_{FFT} \\ 0 & \text{otherwise} \end{cases} \quad (3)$$

To avoid inter-symbol interference (ISI), a cyclic prefix (CP) of length of N_{CP} is pre-appended to each $\boldsymbol{z_i}$ block. Therefore the total number of time domain samples of each OFDM symbol duration is $N_T = N_{FFT} + N_{CP}$. Samples of each OFDM symbol are passed to the Digital to Analog Converter (DAC), up-converted to the carrier frequency f_c, and transmitted over the channel.

B. Receiver

Receiving node downconverts the signal to baseband and digitizes using Analog to Digital Converter (ADC). It then uses short training sequence to perform block boundary detection and coarse frequency offset estimation. It then uses long training field for channel estimation and fine timing/frequency offset estimation. The length of the guard period is a function of the maximum allowable drift in time and frequency. In the short preamble, short, repetitive, uncorrelated training sequences are used by each node to identify the frame start position associated with each signal component. In contrast, long training sequences are identical.

C. Channel Model

Figure 2 illustrates the channel model used for simulation purposes to represent both SOI and SI propagation. SOI channel, h^{soi}, is modeled to reflect path loss and Rayleigh fading effects. Since received packets are transmitted by nodes, randomly located in the cell, h^{soi} is modeled to reflect random discontinuity of SOI channel from packet to packet. SOI is impacted by carrier frequency offset and sampling time offset due to the local oscillator (LO) mismatch Δf_c. CFO can be modeled as a constant positive or negative frequency shift. STO is modeled as fractional delay filter, which applies time-varying lead or lag.

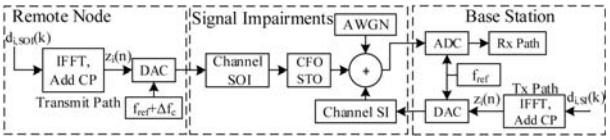

Fig. 2: OFDM transmit path model with signal impairments.

The SI channel, h_{si}, is modeled to reflect path loss and Rayleigh fading effects. Because of fixed relative position of self-interference Tx and Rx antennas, h_{si} is modeled to maintain channel continuity from packet to packet. In addition, it assumes the use of passive self interference suppression due to the use of re-configurable directional antenna at the receive port as described in [1]. The SI signal does not experience either CFO or STO because both the transmitter and receiver are co-located at the base station and share the same clock frequency. Finally, AWGN is added to the composite signal containing a superposition of the two signals.

III. Channel and Synchronization Effects

Each wireless node generates its own clock signal locally. No matter how accurate two asynchronous clock generators are, the frequency of their oscillations will not be exactly similiar. Clock frequency mismatch causes local oscillator frequency mismatch Δf_c between transmitter's LO and receiver's

LO. As a result received signal will experience CFO. The DAC at transmitter and the ADC at the receiver are also driven by asynchronously generated clock signals, thus, after digitization, the received signal samples will experience STO as well. Each signal component in $r(t)$ shown in (1) is subject to time and/or frequency offsets with different amounts, since received signal by BS consists of two signal components transmitted by two different transmitters. SOI component in received signal $r(t)$ is transmitted by remote node and thus, it will be impacted by CFO, STO as well as channel delay. SI component in received signal $r(t)$ is transmitted by BS, therefore it will only experience channel delay. To capture time and frequency misalignments, the received i^{th} block of data $\boldsymbol{r_i}$ can be written as

$$\begin{aligned} r_i(n) = e^{\frac{j2\pi\varepsilon n}{N_{FFT}}} s_i^{tx}(n-\theta) * h_i^{soi}(n) \\ + y_i^{tx}(n-\tau) * h_i^{si}(n) + w(n) \end{aligned} \tag{4}$$

where $s^{tx}(t)$ and $y^{tx}(t)$ are SOI and SI components of the transmitted signal. $h^{soi}(n)$ and $h^{si}(n)$ represent path loss and fading of SOI and SI channels respectively. ε is the relative carrier frequency error, defined as $\varepsilon = \Delta f_c/\Delta f$, θ represents time shift of SOI due to STO plus channel delay, and τ represents time shift of SI due to channel delay. Time offset θ is a gradually increasing quantity, which can have integer, as well as, fraction parts $\theta = \theta_{in} + \theta_{fr}$. Offset τ is relatively constant and can be treated as an integer quantity.

IV. Block Boundary Synchronization Issues

Sampling time offset adds/removes fractional samples to the received signal creating drift in time and causing inter-carrier interference (ICI). Accumulating fractional samples over time result in integer sample shifts creating symbol timing offset, which causes ISI, due to the incorrect placement of the FFT window [2]. In the following, we first consider the effect of STO on the FD system, where $\Delta f_c = 0$ in (4). Under this condition (4) can be rewritten as

$$r_i(n) = s_i^{tx}(n-\theta) * h_{soi}(n) + y_i^{tx}(n-\tau) * h_{si}(n) + w(n)\ . \tag{5}$$

In order to perform digital cancellation of SI and extract data from SOI, it is essential to locate the edges of both signal components and compensate for their offsets.

In general, to locate the edge of a frame, receiver correlates the received signal with locally stored copy of short training signal and searches for the peak position.

$$\hat{\rho} = \arg\max_n \Big[\sum_{m=1}^{W_d} r_i(m) \cdot p^*(m+n) \Big] \tag{6}$$

where ρ is detected peak position, W_d is correlation window width and $p(n)$ is the local copy of short training. However, correlation and peak position detection approach alone can easily lead to incorrect results in FD mode, due to the fact that two adjacent short training fields in received signal are subject to different impairments. To analyze the failure of conventional edge detection approach in details, we will look into the following scenarios, that occur frequently in FD mode.

Scenario 1: Overlap of SI and SOI short trainings in received signal. Time drift can shift SOI component in time causing short training field to overlap with SI short training filed in received signal. The overlapping region represents the sum of SOI and SI, which occurs when $\tau - \theta < N_T$.

$$\hat{\rho} = \arg\max_n \Big[\sum_{m=1}^{W_d} [s_i^{rx}(n-\theta) + y_i^{rx}(n-\tau)] \cdot p^*(m+n) \Big] \tag{7}$$

Correlation with overlapped region has potential of resulting in large false peaks.

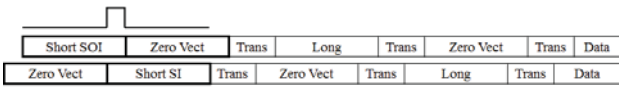

Fig. 3: Overlap of short training fields in FD OFDM frame.

Scenario 2: Large power difference between SI and SOI components in received signal, in the absence of overlap $\tau - \theta > N_T$. Due to the fact that SI transmit antenna is located very close to Rx antenna, received SI short training power can be much larger than SOI short training power. In that case correlation of received SI with SOI local copy will still result in uncorrelated signal with high enough peaks, located next to SOI short training field. Those false peaks can mislead peak detection algorithm into detecting wrong edge.

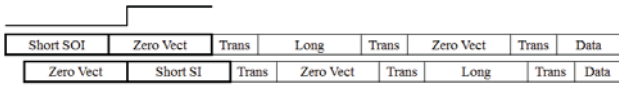

Fig. 4: FD OFDM frame with large power of SI short training.

Note that inserting zero padded guard interval between short training fields helps with block boundary detection in Scenario 1, but it does not help in Scenario 2. Hence we propose the following technique that combats false correlation peaks in both cases.

V. Proposed Synchronization Techique

First, the receiver aims to locate the boundary of SI, which is obvious to locate, due to the fact that SI component experiences a fixed propagation delay without any time drift and has significant power after ADC. To estimate $\hat{\tau}$, receiver cross-correlates the local copy of SI training sequence with received signal $r(n)$, and searches for peak position as described below

$$\hat{\tau} = \arg\max_n \Big[\sum_{m=1}^{W_d} r(m) \cdot p_{si}^*(m+n) \Big] \tag{8}$$

where $p_{si}(n)$ is the local copy of SI short trainings. Once SI boundary location is found, receiver estimates SI channel $\hat{H}_{si}(k)$, and uses it to perform digital cancellation on SI short training effectively removing it

$$g(n) = r(n) - p_{si}(n-\hat{\tau}) * \hat{h}_{si}(n). \tag{9}$$

where $g(n)$ represents a copy of received signal $r(n)$ with SI short training signal removed. Now receiver can safely cross-correlate the local copy of SOI training sequence with the received signal $g(n)$, and search for peak position in order to estimate $\hat{\theta}_{in}$ as described below

$$\hat{\theta}_{in} = \arg\max_n \Big[\sum_{m=1}^{W_d} g(m) \cdot p_{soi}^*(m+n) \Big] \tag{10}$$

Algorithm 1 Robust Block Boundary Detection (RBBD)

1: Detect SI boundary by estimating $\hat{\tau}$
2: Extract SI Long Training use $\hat{\tau}$
3: Estimate SI Channel $\hat{h}_{si}(n)$ use SI Long Training
4: Construct Rx SI short training $\hat{y}_i(n) = p_{si}(n-\hat{\tau}) * \hat{h}_{si}(n)$
5: Subtract $\hat{y}_i(n)$ from received signal$\rightarrow$ $g(n) = r_i(n) - \hat{y}_i(n)$
6: Detect SOI boundary using $g(n)$ by estimating $\hat{\theta}$

where $p_{soi}(n)$ is the local copy of SOI short training. The correlation window width W_d dictates that the synchronization error must be within a tolerable range. For that reason the receiver must exploit a pilot signal transmitted by the transmitter and readjust transmission start time.

The benefit of the presented technique is twofold. Not only does it introduce robustness in block boundary detection, but also contributes in frequency offset estimation. Since short training is also used for coarse frequency offset estimation, overlapping short training fields in received signal $r(n)$ (Scenario 1) will cause a large CFO estimation error. However, cancellation of SI short training for RBBD purposes results in signal $g(n)$, which has SI free short training field and can be used for coarse frequency offset estimation.

Figure 5 illustrates the block diagram of an OFDM receiver supporting IBFD synchronization. The shaded blocks in the figure indicate processing steps that are novel to this architecture as opposed to a standard OFDM receiver. A key difference in this architecture is that block boundary detection of SOI and coarse frequency offset estimation is performed after SI short training removal.

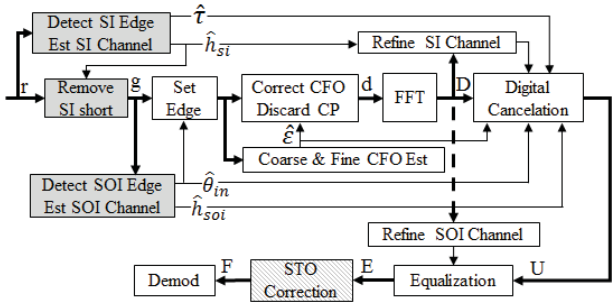

Fig. 5: OFDM receiver diagram with IBFD synchronization.

VI. Experimental Results

The proposed technique has been experimentally tested on an FD system with timing and frequency offsets. The experimental FD platform consists of software defined radios (SDR) operating in the topology shown in figure 1. All SDRs parameters are set according to signal parameters listed in Table I.

Figure 6 represents a snapshot of a received frame preamble, where SOI and SI short training parts experience partial overlap corresponding to Scenario 1 in Section IV. Figure 7 represents a snapshot of a received frame preamble, where SOI and SI short training parts do not overlap, but magnitude of SI is larger then SOI, which corresponds to Scenario 2. Frame

OFDM Parameters	Value	Signal Parameters	Value
Number of OFDM Subcarriers	64	Sim. Channel Type	D
Number of Pilots	4	AWGN Power	-100 dBm
Cyclic Prefix (CP)	$3.2\mu s$	Rx SOI Power	-70 dBm
Symbol Duration (CP+FFT)	$16\mu s$	Carrier Frequency	2.5 GHz
Short Training Duration	$16\mu s$	Signal Bandwidth	5 MHz
Subcarrier Frequency Spacing	78125Hz	Tx Power	5 dBm

TABLE I: Simulation and Experiment parameters.

boundary detection alone failed to detect corrected frame start position in both cases.

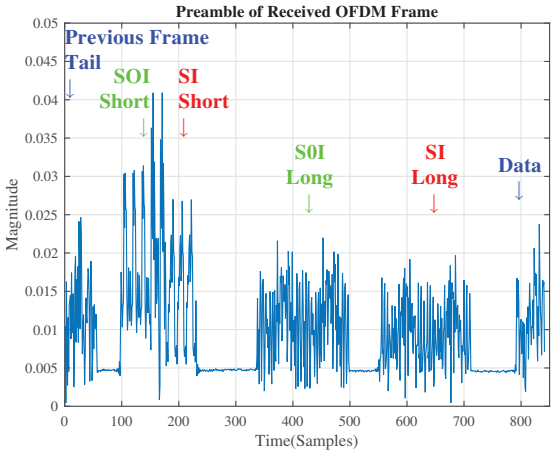

Fig. 6: Received OFDM frame with partially overlapped SI and SOI short preambles (Scenario 1).

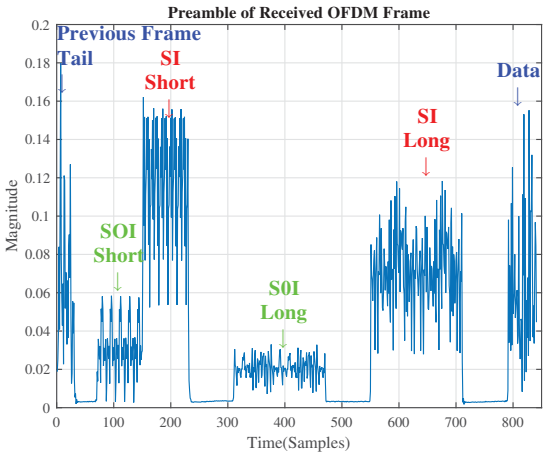

Fig. 7: Received OFDM Frame with SI larger than SOI (Scenario 2).

The proposed RBBD algorithm manages to suppress SI short preamble down to the noise floor and increases the probability of correct SOI edge detection as well as coarse CFO estimation as shown in Figure 8. Note that suppression of SI short preamble depends on the accuracy of SI channel estimate, and does not depend on the the type of occurred scenarios.

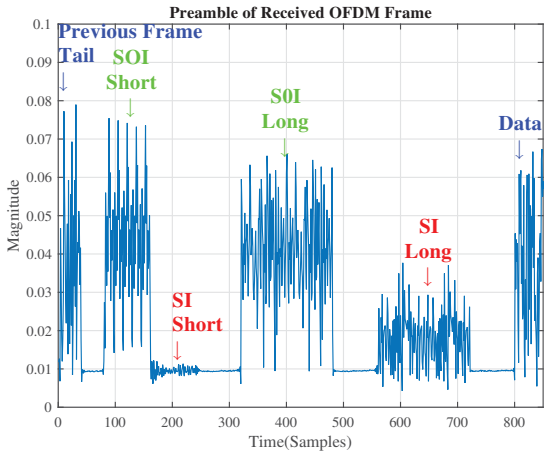

Fig. 8: Rx OFDM Frame after removal of SI short preamble.

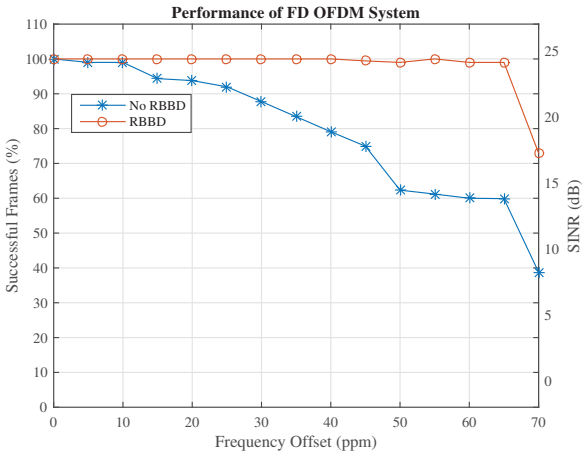

Fig. 9: Performance of the FD system vs. CFO.

VII. Simulation Results

To further highlight the benefit of RBBD, the FD system in figure 1 was simulated for large values of CFO and various SI suppression values. All simulations are performed according to the parameters listed in Table I. Overall performance of FD system with and without RBBD is plotted in figures 9 and 10.

Figure 9 illustrates successful frame reception rate as a function of CFO while SI power is kept constant at -75dBm. The large value of cancellation is necessary to show how non-RBBD approaches fail. The figure compares the performance of the system under Scenario 1, since the length of the overlapping interval is proportional to the rate of time drift. From the figure 9 it becomes clear that successful frame reception rate of a system without RBBD drops as CFO increases. However when RBBD is applied, the system provides frame success rate of 100% up to CFO of 65ppm. The figure also shows the average system SINR of the received signal at SOI demodulation step.

Figure 10 illustrates successful frame reception rate as a function of SI suppression level before ADC, while CFO is kept constant at 1ppm. This corresponds to Scenario 2. From figure 10 one can see that the system without RBBD is doing well up to SI suppression of 75dB. This corresponds to the SI power of -70dBm, which equals to SOI power. Increasing SI power more causes block boundary detection errors and a large drop in performance. In case of RBBD the system can withstand large SI levels up to -30dBm and still provide successful frame reception.

VIII. Conclusion

This paper presents robust block boundary synchronization for in-band full-duplex OFDM system. Detection of frame boundary is one of the initial steps towards successful demodulation of OFDM data. Inaccurate block boundary estimation leads to the loss of the whole data block. Two common failure scenarios are discussed and a novel, robust approach is presented, which boosts synchronization performance and allows operation in severe channel conditions. Simulation and experimental results are presented showing the effectiveness of the proposed technique.

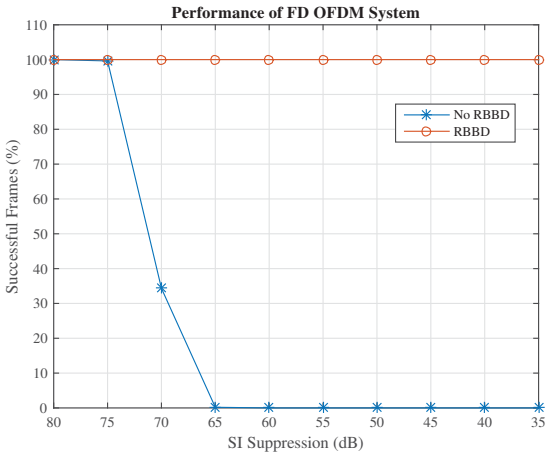

Fig. 10: Performance of the FD system vs. SI suppression.

Acknowledgment

The authors gratefully acknowledge support from the National Science Foundation under award number 1710746.

References

[1] Sergey Shaboyan, Elsayed Ahmed, Alireza S Behbahani, Waleed Younis, and Ahmed M Eltawil. "Frequency and Timing Synchronization for In-Band Full-Duplex OFDM System". In *GLOBECOM*, 2017.

[2] H. Lee, J. Choi, D. Kim, and D. Hong. "Impact of time and frequency misalignments in OFDM based in-band full-duplex systems". *IEEE WCNC*, pages 1–6, 2017.

[3] J. Choi, D. Kim, S. Lee, H. Lee, J. Bang, and D. Hong. "A new frame structure for asynchronous in-band full-duplex systems". *IEEE PIMRC*, 2015-Decem:487–491, 2015.

[4] Sergey Shaboyan, Alireza S. Behbahani, and Ahmed M. Eltawil. "Active Cancellation of Self-Interference for Full-Duplex Amplify and Forward Wi-Fi Relay", 2018.

[5] IEEE Computer Society. "IEEE Standard -Specific requirements - Part 11: Wireless LAN Medium Access Control (MAC) and Physical Layer (PHY) Specifications. *IEEE Std 802.11-2016 (Revision of IEEE Std 802.11-2012)*, 2016(June):1–3534, 2016.